Desalination and Water Treatment
www.deswater.com

doi:10.5004/dwt.2019.23748

148 (2019) 42–50
April

A new biomimetic aquaporin thin film composite membrane for forward osmosis: Characterization and performance assessment

Soleyman Sahebi[a,b,*], Mohammad Sheikhi[c], Bahman Ramavandi[d,e]

[a]*Department for Management of Science and Technology Development, Ton Duc Thang University, Ho Chi Minh City, Vietnam, Mobile: +989039839553, email: soleyman.sahebi@tdtu.edu.vn (S. Sahebi)*
[b]*Faculty of Environment and Labor Safety, Ton Duc Thang University, Ho Chi Minh City, Vietnam*
[c]*Research and Technology Center of Membrane Processes (RTCMP), School of Chemical, Petroleum and Gas Engineering, Iran, University of Science and Technology (IUST), Narmak, Tehran, Iran, Mobile: +989386824944, email: Sheikhi.moh@gmail.com (M. Sheikhi)*
[d]*Environmental Health Engineering Department, Faculty of Health and Nutrition, Bushehr University of Medical Sciences, Bushehr, Iran, email: ramavandi_b@yahoo.com (B. Ramavandi)*
[e]*Systems Environmental Health and Energy Research Center, The Persian Gulf Biomedical Sciences Research Institute, Bushehr University of Medical Sciences, Bushehr, Iran*

Received 28 July 2018; Accepted 2 January 2019

ABSTRACT

Cellulose acetate (CA) and thin film composite (TFC) membranes for forward osmosis (FO) process by hydration technology innovations (HTI) were the most innovative and also commercialized for research and field scale. Most recently, biomimetic Aquaporin (AQP) membrane has been commercialized on a large scale and product outlet is available for industrial and academic applications. In this work, we present the characterization and evaluating the performance of the biomimetic AQP forward osmosis (FO) membrane from aquaporin Asia Pte. Ltd in Singapore, using DI water and brackish water (BW) (5000 mg·L^{-1} of KCl) as feeds and KCl as draw solution (DS). Scanning electron microscopy (SEM), atomic force microscopy (AFM), Fourier-transform-infrared (FTIR), and contact angle analysis were utilized to characterize AQP membrane. The intrinsic properties of the membrane were also assessed using a reverse osmosis (RO) setup followed by investigating FO performance in a lab-scale FO setup. Under FO tests, the membrane achieved high water flux of 12.8 and 17.1 L m^{-2} h^{-1} with a modest RSF of 14.8 and 17.5 g m^{-2} h^{-1} using 1.0 M KCl against DI water in FO and pressure retarded osmosis (PRO) modes, respectively. The results were also equaled to 9.1 and 10.1 L m^{-2} h^{-1} of water flux under FO and PRO modes as BW was used as FS.

Keywords: Biomimetic aquaporin; Forward osmosis; Non-woven backing fabric; Thin film composite

1. Introduction

Forward osmosis (FO) is a promising membrane approach that allows water permeation from a low concentrated solution, named feed solution (FS) towards a high concentrated solution, named draw solution (DS) across the semi permeable membrane under the influence of inherent osmotic pressure gradient of an osmotic agent [1,2]. Accordingly, operating FO systems demands no or technically low applied hydraulic pressure, which provides the capability of water reclamation, brine dewatering [3–5] and concentrating saline waters or FSs with the potential of low fouling tendency [6–8]. Moreover, this inspired industries to employ FO technology in power generation [9], landfill leachate treatment [10], liquid foods treatment [11], and farm irrigation [12–14] disciplines.

Current membrane developments for FO progress are focused on fabrication of thin film composite (TFC) membrane platform, which includes a thin selective layer that is formed on the top of a porous support material through interfacial polymerization (IP) approach [15–18]. However, there are studies on the literature around development and application of neat cellulose acetate based hollow fiber

*Corresponding author.

nanofiltration (NF) and fabrication of double-skin membranes for FO applications [19,20]. Majority of the studies regarding this platform can be divided into two particular categories. First, support layer optimization in the term of the structural parameter (S value) to achieve a membrane support layer with less internal concentration polarization (ICP), which is broadly regarded as the preliminary factor for low FO membrane performance [21,22]. Furthermore, despite external concentration polarization (ECP), which can be handled by the mean of hydrodynamic operating conditions, ICP has been noticed as the major hindrances on the way of membrane development for FO process, as it happens in the membrane inner side of support layer [23]. For achieving less ICP, recent attempts focused on further improvement of the support layer with lower S parameter, which can be achieved by improving porosity or reducing tortuosity and membrane thickness [22]. The results of this improvement were also led to fabrication of an asymmetric membrane constructed from cellulose triacetate (CTA) on a backing fabric by Fluid Technology Solutions (FTS, formerly Hydration Technology Innovations, HTI) company (Albany, OR, USA) in industrial scales [24,25]. Although the membrane, which was firstly developed by HTI did not exhibit wonderful enough performances, HTI and few other companies recently made on a full-scale production for thin film composite (TFC) FO membrane with higher performance in the terms of water flux, slat flux and rejection [24,26].

The second category, which is responsible for desalination and salt ions rejection includes enhancing the selective layer of TFC membranes. It is noteworthy to outline that this area has not attracted considerable attention of the researchers compared to that of the support layer due to limited capable materials that are feasible to participate in IP [27,28]. In other words, common RO-type approaches for formation of the rejection layer via IP have been broadly chosen in this field. However, there are reports around top layer modifications that are relied on polycondensation reactions between aqueous and organic phases of amine and acid chloride, respectively [29]. Lately, incorporating hydrophilic nanoparticles (NPs) into the selective layer was introduced as an alternative to evolve applicable membranes with higher performances compared to other typical RO-type membranes. Many reports are available on literature that investigate addition of hydrophilic NPs such as NaY zeolites [30], functionalized silica nanoparticles [31,32], functionalized and non-functionalized carbon nanotubes [33,34], and titanate nanotubes [35]. To the best of our knowledge, none of the above mentioned NPs incorporated membranes (named nano-composite or mixed matrix membranes) have not the chance of assimilating into the commercialized membrane categories.

In the course of modifying FO membranes, the discipline of protein-based biomimetic membranes, which can be regarded as biomimetic-hybrid membranes, has attracted a significant attention. Biomimetic membranes were developed by reconstituting biological membrane proteins into the artificial lipid bilayers, block copolymers (BCP) or frigid nanopores [26]. Significant advantages such as high water permeability and smart selectivity characteristics have pushed researchers to investigate incorporating water channel membrane proteins, named aquaporin (AQP), into the membrane substrate [29]. The researches regarding the aquaporin-based hybrid membranes have just increased expeditiously, in a way that some of them have estimated water permeability augment to values up to 2 folds of the commercial desalination membranes and selectivity move towards 100% [36]. Aquaporin (AQP) is a pore-forming protein that forms channels within the selective layer that allows water to permeate and reject salt ions species under application of appropriate conditions [37–39]. This innovative concept was firstly launched by Jensen et al., which was followed by published by Kumar et al. implying reconstitution of functional AQP in BCPs [40].

Despite indisputable characteristics of AQP as a starting material for next-generation of membrane separation technologies, numerous challenges such as stability under influence of saline or high foulants content feeds, and production in large scales are still maintained a concern [41]. These questions pushed researches to address fabrication of AQP incorporated membranes challenges. Sun et al. utilized fabricated and characterized addition of AqpZ planar lipid bilayers employing Langmuir–Blodgett transfer while nickel-chelating lipids were also considered as one lipid blend component [42]. Although among the utilized strategies of fabricating mentioned membranes, functional AQP vesicles deposition on porous supports are the most considered method, constructing free-standing lipid without supports are also reported [43–47]. However, applying these methods did not exhibit desirable results in the terms of water flux and salt rejection [45,46,48]. Accordingly, various approaches have been investigated to improve either deposition or immobilization of vesicles on the porous support layer. The mentioned methods are comprised of direct deposition of vesicle onto the substrates, charge induced vesicle adsorption [43,49], pressure assisted vesicle fusion [43,44,50], magnetically improved vesicle deposition [44], and chemical crosslinking functionalized lipid/polymer and the support [44,51].

The main aim of the current study is to evaluate and characterize a newly commercialized FO AQP membrane. Firstly, the AQP membrane was characterized by the mean of scanning electron microscope (SEM), atomic force microscopy (AFM), contact angle and Fourier-transform-infrared spectroscopy (FTIR) analysis. Moreover, the intrinsic separation properties of the membrane such as water permeability coefficient (A), salt permeability coefficient (B), salt rejection (R_s) and structural parameter were also evaluated. Furthermore, FO performance was evaluated and compared with current commercialized FO membranes.

2. Materials and methods

2.1. Membrane, feed and draw solution

A newly commercialized aquaporin-incorporated FO TFC flat-sheet membranes (Aquaporin Asia Pte. Ltd., Singapore), with the reported Calcein rejection of >99.0% ±0.5% by the manufacturer, were used in all of the experiments. The membranes were stored at ambient temperature and got immersed in deionized water (DI) virtually 30 min before use.

Potassium chloride (KCl) were obtained from Merck and used for DS and brackish water (BW) preparation. Four concentrations of DS (0.5, 1.0, 2.0 and 3.0 M) were considered as DS to provide osmotic pressure. Moreover, DI water,

and a brackish water including 5 g·L^{-1} of KCl, which was named as BW5, were employed as FS.

2.2. Membrane characterization

Morphology of cross section and top surface of the membrane were investigated utilizing a high-resolution VEGA\\TESCAN scanning electron microscope. The membrane samples were firstly freeze dried and then the dried samples were firstly immersed in liquid nitrogen for few seconds, then it was cut by sharp razor blade for easer break due to membrane non-woven backing support [16]. Later on, the broken membrane was coated with an ultra-thin layer of gold exploiting Blazers Sputter coater (SCD 050, BAL-TEC, Germany) to be prepared for imaging.

Atomic force microscopy (AFM, ICON Veeco) in the tapping mode under ambient conditions was used to evaluate roughness of the membrane surface. Fourier-transform-infrared spectroscopy (FTIR) was carried out utilizing an FTIR spectrometer PerkinElmer (Waltham, MA, USA) Spectrum RX1 in the range of 650 to 4400 cm^{-1} to evaluate the functional groups and indicate chemical characteristics of the AQ membrane. Thickness of the membrane was assessed using a digital micrometer (293–330 Mitutoyo, Japan). Archimedes' principle was used to measure the membrane porosity (ε) based on the following equation:

$$\varepsilon = \frac{(Ww - Wd)/\rho i}{\left[\frac{Ww - Wd}{\rho i}\right], + \left[Wd/\rho p\right]} \times 100\% \tag{1}$$

where W_w is wet mass and W_d is dry mass of the membrane. ρ_i and ρ_m are also densities of the wetting solvent and the membrane, respectively.

Sessile drop contact angle (Contact Angle System OCA20, Dataphysics Co., Germany) was exploited to calculate hydrophilicity of the top and the back surfaces of the air-dried AQ membrane. Contact angle was assessed using 5 µL probe DI samples recorded at 23°C and 30% relative humidity.

2.3. Assessment of membrane's structural and separation properties

An RO setup was utilized to evaluate membrane's water permeability coefficient (A) at applied hydraulic pressures on the range of 0 to 5 bar with the same membrane module that was used. Furthermore, salt rejection (R_s) was also determined according to our previous paper [16] considering 200 mg·L^{-1} of KCl as feed at 1.0 bar applied pressure employing calibration method based on conductivity measurements [Eq. (2)]. Salt permeability coefficient (B) was later utilized by the bellow relationship [3]:

$$R_s(\%) = \left(1 - \frac{C_p}{C_f}\right) \times 100 \tag{2}$$

$$\frac{1 - R_s}{R_s} = \frac{1}{(\Delta P - \Delta\pi)A} B \tag{3}$$

where C_p and C_f are concentrations of NaCl in the feed and the permeate, respectively. Δπ is net osmotic pressure gradient of the feed and the permeate flows and ΔP is applied hydraulic pressure gradient.

S value as one of the most defining characteristics of TFC-FO membranes can be calculated using the following equation based on support layer thickness (t), tortuosity (τ) and porosity (ε):

$$S = \frac{t\tau}{\varepsilon} \tag{4}$$

The effective structural parameter was assessed experimentally using the classical ICP model developed by Loeb et al. [52] according to the following correlation:

$$J_w = \frac{D}{S}\left[\ln\frac{A\pi_{D,b} + B}{A\pi_{F,b} + Jw + B}\right] \tag{5}$$

where J_w, D, B, $\pi_{F,b}$ and $\pi_{D,b}$ are WF, bulk diffusion coefficient of the DS, salt permeability coefficient of the membrane active layer, bulk osmotic pressures of the FS and the DS, respectively. According to Eq. (5), the S value is calculated utilizing the following relationship:

$$S = \left(\frac{Ds}{J_w}\right)\ln\frac{A\pi_{D,b} + B}{A\pi_{F,b} + J_w + B} \tag{6}$$

2.4. FO experimental setup and testing procedure

A lab-scale FO setup was utilized to evaluate AQP-flat-sheet FO membrane performance in the terms of WF (J_w), reverse solute flux (RSF) and special reverse solute flux (SRSF). The setup includes an FO process cell with the length, width and depth as 3.1 cm, 2.0 cm and 0.3 cm, respectively, which provides an effective surface area of 6.2 cm^2. Four pressure transmitters, installed before and after the membrane cell on the path of FS and DS flows. Moreover, a temperature transmitter within the FS and DS reservoirs were also utilized to monitor operating parameters. FS and DS were pumped through the membrane channels by the mean of a two-way pump (Pumpdrive 5001, Heidolph-Germany) with equal volumetric flow rates of 400 ml·min^{-1}. The experiments were carried out in both FO (active layer faced FS) and PRO (active layer faced DS) modes to better understand the membrane performance and effects of ICP. Moreover, the experiments were initiated with equal loaded volume as 250 ml of both FS and DS reservoirs and continued for 30 min. J_w was assessed by measuring DS weight change through the following equation:

$$J_w = \frac{\Delta m / \rho_{feed}}{Sm\Delta t} \tag{7}$$

where Δm, S_m, ρ_{feed} and Δt are DS mass variation as it increases during the tests (kg), effective membrane area (m^2), runtime (h) and water density at 25°C, respectively. In order to calculate RSF (J_s) DI water was firstly pumped as FS and various concentrations of KCl (0.5, 1.0, 2.0 and 3.0 M) were considered as DS as well. After each experiments finished, electrical conductivity (EC) of the FS was measured employing a multimeter (Lutron-CD4303, Germany). J_s was evaluated using the following formula:

$$J_s = \frac{C_f m_f}{\rho_{feed} S m \Delta t} \tag{8}$$

where J_s, C_f, and m_f are RFS (g·m^{-2} h^{-1}), KCl concentration in the FS and feed final mass, respectively. Furthermore, SRSF is defined as ratio of RSF to WF as illustrated in the following formula:

$$SRSF = \frac{J_S}{J_W} \tag{9}$$

3. Results and discussion

3.1. Substrate characterization

Morphologies of cross-section, top and back surfaces of the AQP membrane were studied by the mean of SEM, which are shown in Fig. 1. Fig. 1a presents the cross-section image of the AQP membrane. As it is shown, the substrate is highly porous,which includes a large number of finger-like pores that can provide easy water permeation and lower ICP [16]. Fig. 1b shows a closer look of cross-section near the membrane surface, which reveals a high porous sublayer as well. Based on ternary phase diagrams, this means an excellent balance of solvent-polymer-nonsolvent carried out in phase inversion to customize an appropriate membrane for FO process. Further, the sublayer support pores get more aligned as they are close to the top surface that means lower tortuosity and less resistance on the way of water permeation across the membrane. However, the thick support layers can provide high mechanical strength, which leads to maintaining membrane structure and pore shape under the influence of compaction [16].

Fig. 1c shows the morphology of the membrane top surface that is formed by AQP proteins is significantly similar to that of TFC membranes in terms of landscape with hills and valleys topology, which resemble a rocky road. Furthermore, the membrane top surface seems to have high roughness, which may lead eyesight to increase potential of substantial fouling [29]. The back surface of the AQP membrane is also illustrated in Fig. 1d. It shows that the membrane has embedded on nonwoven backing fabric support, which has dramatic roughness that may lead to reduction in concentration polarization (CP) due to substrate engagement with polymeric materials and causing lower side of polymeric support to become more porous during phase inversion [16] (Figs. 1a and d).

The atomic force microscopy (AFM) spectra conducted for AQP membrane is three dimensions which is illustrated in Fig. 2. AFM analysis was performed and depicted in 5

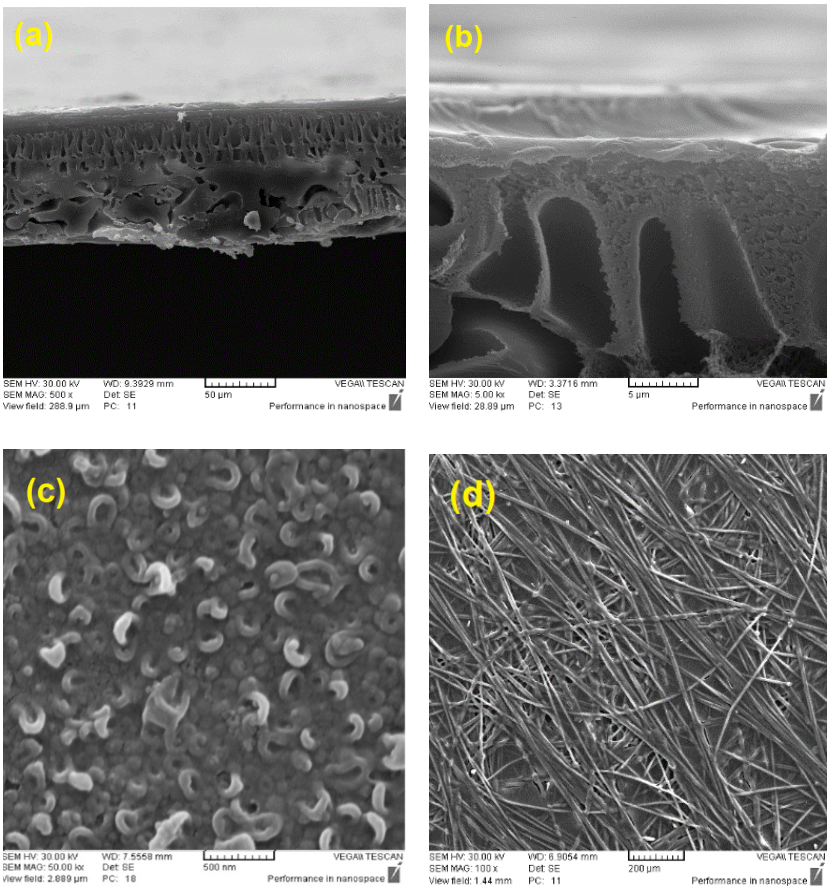

Fig. 1. SEM images of Aquaporin FO membrane a) cross-section, b) cross-section in closer look, c) top surface rejection layer, d) bottom surface nonwoven backing fabric support.

μm dimension to better understand the roughness of the selective layer that was mentioned before as the rough surface with the potential of fouling. Thus R_a, R_p and R_q are also shown in Table 1.

The results show that mean roughness of the AQP membrane's top surface, which is also known as deviation of the surface heights is 61.64 nm. This number is found to be in the range of typical commercial TFC membranes [51]. However, the R_p value, the maximum height of the surface is equaled to 170.65 nm indicating the AQP membrane is prone to fouling if highly foulants feed introduce the surface [29]. The R_q factor also shows the distance between the peeks on the AQP membrane surface. This parameter is equaled to 72.06 nm that indicates the frilly uniform surface. Additionally, AQP proteins have small size whereas the rejection layer typically is 200 nm, which means incorporated AQP proteins may vanish and embed within the polymer matrix [53]. Moreover, by comparing with previous studies and based on SEM images, it can be understood that there is virtually no difference between TFC rejection layers of AQP membranes and prevalent TFC FO membranes [54,55].

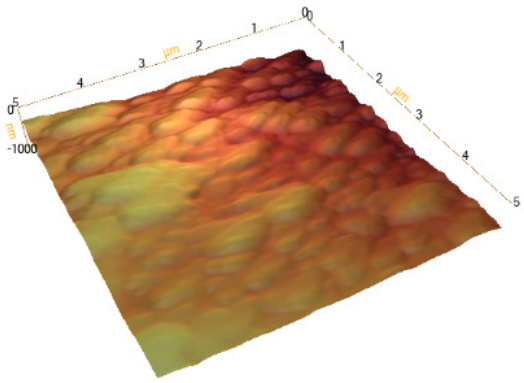

Fig. 2. AFM image of the AQP membrane.

Table 1
AFM parameters of AQP membrane

Sample	AQP
Ra (nm)	61.64
Rp (nm)	170.65
Rq (nm)	72.06

As it was outlined before, contact angles of the top and bottom surfaces of the AQP membrane was measured to investigate its hydrophilicity. Table 2 presents a comparison between the top and back surfaces' contact angles of the AQP membrane and those of HTI-CTA and TFC membranes. As can be seen, the active layer of the AQP membrane has a lower contact angle compared to that of the support layer, which may be attributed to the characteristics of the rejection layer [29]. Furthermore, a nonwoven fabric has been used as support for this membrane. Then, unlike FO CTA membrane, which has similar materials on both sides due to polymer solution penetration related to the woven mesh fabric, in AQP membranes, it seems the polymer did not penetrate the fabric. The nonwoven used for AQP membrane is similar with TFC RO membrane with lower thickness.

Fig. 3 shows the FTIR analysis of the AQP membrane. As represented in the chart, there are numerous organic and inorganic bonds signs that have shown up. Based on FTIR data and by comparing them with FTIR of polysulfone (PSf) and polyethersulfone (PES), it was realized that the membrane support is some kind of PSf, or PES that is modified with pore formers such as polyvinylpyrrolidone (PVP) or polyethylene glycol (PEG). According to stretching vibration occurs at 1323.99 cm^{-1}, 1294.79 cm^{-1}, 1241.85 cm^{-1} and 1169.77 cm^{-1} are related to a symmetric stretch of the sulfone group (SO_2 and SO). Moreover, the peaks at 1541 cm^{-1} and 1649 cm^{-1} are contributed to the vibration of –NH and –CONH–, respectively, which is related to the protein molecules. It was realized that the peaks at 3100 cm^{-1} to 3600 cm^{-1} are related to the existence of PEG or PVP molecules in the support layer.

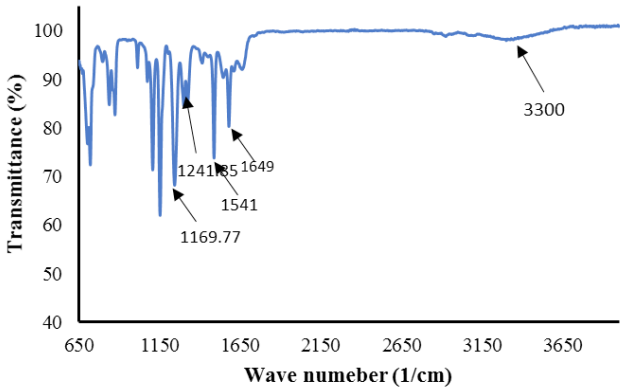

Fig. 3. FTIR spectra of the AQP membrane on the range of 650 cm^{-1} to 4000 cm^{-1}.

Table 2
Characteristics comparison of AQP membrane with HTI CTA and TFC membranes

Sample ID	Thickness (μm)	Porosity (%)	Contact angle (°)		Ref
			Active layer	Support layer	
HTI CTA	93 ± 3.0	N/A	76.6 ± 0.5	81.8 ± 0.5	[56]
TFC	148 ± 1.0	N/A	14.3 ± 1.6	*N/A	[29]
AQPs	132 ± 3.0	65 ± 1	50.3 ± 0.5	74.8 ± 0.5	Current study

*N/A: not available.

3.2. Intrinsic properties of AQP membrane

Apart from the properties of the selective layer, previous studies showed that the substrate construction has a significant impact on the performance of the membrane [15]. In other words, researchers have tried to develop an ideal membrane based on lower structural parameter (S) values [24,57], in a way that the lower *S* value, the higher water flux. However, water permeability, salt rejection and RSF have some kind of trade-off that should be optimized to meet the standard criteria of commercialization [29]. Thus, the intrinsic characteristics and structural properties of the AQPs membrane were evaluated, simultaneously, for the AQP membrane to better understand the influence of substrate structure on the membrane performance (Table 3). As illustrated, AQP membrane has higher A and B values as well as lower R_s compared to those of commercial TFC membranes and tend to a bit increase in *S* value. This may be related to the low stability of AQP proteins towards saline waters [36]. In the course of developing TFC FO membranes, many efforts have been made and the raised challenges towards fabricating better and defect-free membranes have been mostly solved [5,16,18]. However, as the AQP membranes fabrication industry are on the early of its way, many challenges such as membrane stability still remained an issue. Moreover, apart from existence of AQP proteins at the selective layer, higher A value maybe is contributed to the substrate finger-like morphology that allows better permeation of water across the membrane as a result of less hydraulic resistance on the way of water flow [41].

3.3. Forward osmosis performance

FO performance of AQP membrane was evaluated in a lab-scale FO setup in the terms of WF, RSF and SRSF using KCl as DS as well as DI water and 5000 mg·L^{-1} of KCl as DS. The results of the performed experiments in both FO and PRO modes are depicted in Fig. 4. As can be seen, while the DI water was employed as FS the WF and RSF were increased as the DS concentration goes up in both FO and PRO experiment modes. This is attributed to the increased osmotic pressure gradient over the DS side of the membrane that increases driving force of permeating water molecules across the AQP membrane [58,59]. Moreover, WF and RSF exhibit higher amounts as the experiments were carried out in PRO mode compared to those in FO mode owing to significant ICP in FO experiment mode [49,60]. As the FO mode is applied, the salt ions seep through the porous substrate to get the interior surface of the active layer as a result of chemical potential gradient over the membrane sides [3,58]. Thus, the ion concentration is declined under the influence of convection when the water molecules permeate across the membrane and within the porous layer. This brings about KCl ions diffuse back to the interior surface and a significant decline occurs in solute concentration at the active layer to amounts

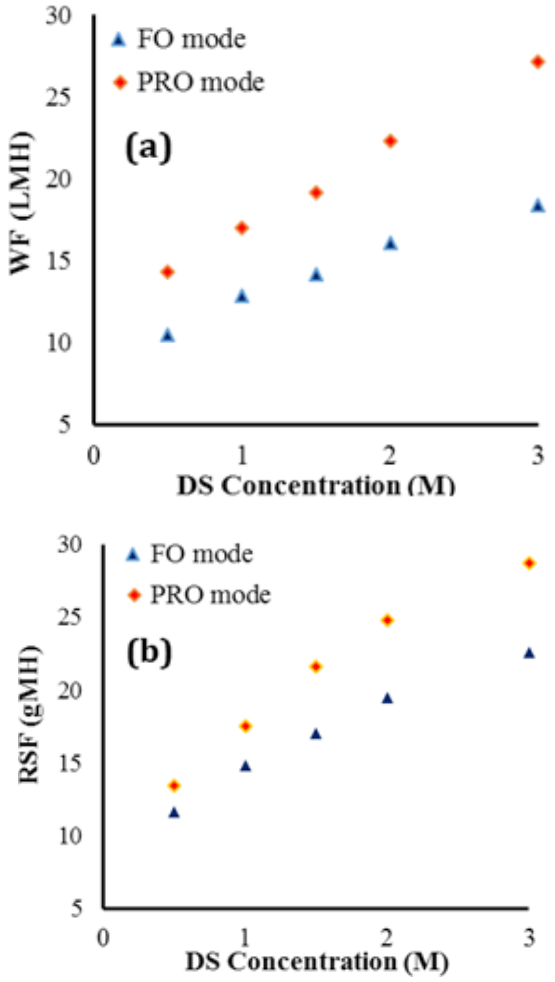

Fig. 4. DS concentrations on performance of AQP membrane in FO and PRO experiment modes using DI water as feed; a) Water flux; b) RSF.

Table 3
Intrinsic properties and structural parameters of AQPs membrane sample

Sample ID	[a]Water permeability (*A*)		[b]Salt permeability *B*	KCl/NaCl rejection (%)	[c]*S* value (μm)	Ref
	L/m^2 h^{-1} bar^{-1}	×10^{-12} m/s Pa	× 10^{-7} m/s			
AQPs	3.1 ± 0.10	8.6 ± 0.15	2.5 ± 0.30	76.3	735	This study
TFC-FO	1.19 ± 0.06	3.18 ± 0.17	0.76 ± 0.13	97.4	492	[15]

[a]calculated in the RO setup at an applied pressure of 1.0 bar with DI water as feed.
[b]calculated in the RO setup at an applied pressure of 1.0 bar with DI water as feed including 200 mg·L^{-1} of KCl.
[c]calculated according to experiments under the FO mode employing 5000 mg·L^{-1} of KCl as the DS with DI water as FS.

much lower than the DS bulk concentration that eventually reduces the water flux [59]. However, considering that the ICP is somehow inherent side effect that coincides with water permeation in all of the FO experiments, AQP membrane exhibited relatively acceptable water flux compared to commercial HTI CTA and TFC membranes [3]. As mentioned before RSF was also increased when PRO experiment is employed. This is contributed to fouling over the membrane owing to cake-enhanced osmotic pressure, which occurs as a result of DS concentration difference across the top layer of the AQP membrane [61]. The obtained data are in good agreement with the previous studies regarding the influence of FO and PRO experiment modes [26,36,59].

SRSF is a metric parameter to quantify and evaluate the DS amount loss per unit of water permeate across the membrane. This valuable parameter is used to compare the FO performance as different membranes, DSs, osmotic agents or FS are under investigation [57]. In other words, the lower SRSF the more desirable FO performance, which means less DS loss and higher WF. As illustrated in Fig. 5 the SRSF goes up as DS concentration increases to the amounts lower than 2 M followed by a decline at the higher concentrations for both FO and PRO modes. However, the difference between FO and PRO mode data is declined as the DS concentration increases until SRSF of PRO mode surpasses the FO mode at DS concentrations higher than 2 M. The obtained data for AQP membrane are in good agreement with previous studies, in a manner that the trend is comparable but not superior to HTI CA and TFC membranes. This means there are many research opportunities to enhance the AQP membranes performance.

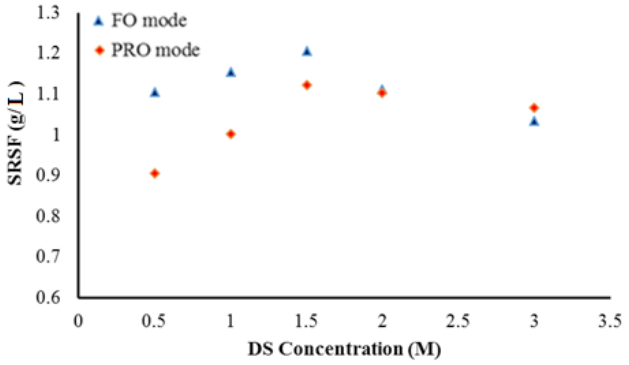

Fig. 5. Effects of the DS concentrations on SRSF of AQP membrane in FO and PRO experiment modes using DI water as feed.

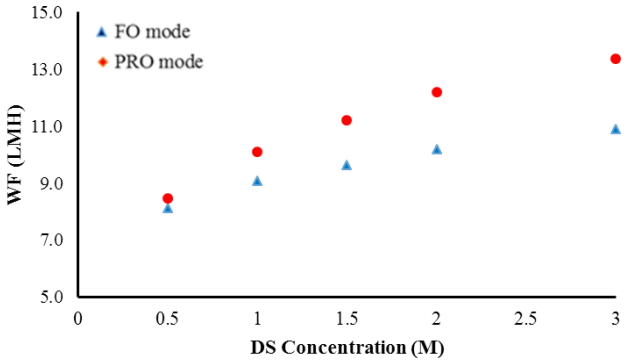

Fig. 6. Effects of the DS concentrations on AQP membrane performance in FO and PRO experiment modes using BW5 as feed; a) WF; b) RSF.

Fig. 6 shows the results of treating BW5 in FO and PRO modes, which contains 5000 mg·L^{-1} of KCl. As it was expectable, although the water flux exhibits a significant decline, the data maintained similar trend in a manner that water flux of PRO mode is higher than that of FO mode similar to experiments performed with DI water as feed. WF has experienced a significant decline due to decreased osmotic pressure gradient over the membrane sides and external CP simultaneously.

Table 4 presents a comparison between the results of the current study with previous studies that have been performed using commercial FO membranes. As can be seen, the AQP membrane investigated in this study exhibited relatively higher water flux than most of the commercial TFC membranes made from CTA. Moreover, it showed lower SRSF compared to CTA and TFC membranes, which may be related to higher WF owing to existence of AQP proteins in its selective layer.

4.Conclusions

In this study, we report the performances and characterizations for the first commercial biomimetic AQPFO membrane, which was supplied by Aquaporin Asia Pte. Ltd in Singapore. The membrane performance does not surpass the available commercial CTA and TFC FO membranes, however, it's admirable to see the further advances in utilizing the AQP proteins for desalination, especially for FO process. Further advancement in this unique TFC membrane for FO process may lead to achieve a membrane with much better results than current FO membranes. This may be the first step in the right direction for development of new generation of smart membranes for water treatment and desalination. Based on natural materials (proteins and lipids) used in the membrane selective layer, life cycle assessment of membrane may play a vital role in application of this unique membrane for practical and large-scale field. In this study, SEM, FTIR, AFM and contact angle analysis were employed to characterize AQP membrane followed by evaluating water and salt permeability, WF and R_s of the AQP membrane in an RO setup. Later on, FO performance was investigated in a lab-scale FO setup. The following summary is achieved from this membrane evaluation:

- SEM and AFM showed that the AQP membrane has the support layer and top rejection layer morphology similar to those of commercial TFC-FO membranes.
- FTIR analysis showed that the substrate material perhaps includes PES that is modified with PEG or PVP copolymers whereas the vibration of –NH and –CONH is related to protein molecules.
- The membrane exhibited high WF of 12.8 and 17.1 L m^{-2} h^{-1} with a modest RSF of 14.8 and 17.5 g m^{-2} h^{-1}utilizing 1.0 M KCl against DI water in FO and PRO modes, respectively.

Table 4
Performance comparison of AQP FO membrane with commercialized flat sheet TFC and CTA membranes

Membrane types	Materials	WF ($Lm^{-2}h^{-1}$)	SRSF ($g\ L^{-1}$)	DS(M)KCL	FS	References
AQP membrane	PES/PEG	12.8/17.1	0.4/0.32	1	DI	Current AQP membrane
CTA flat-sheet (HTI)	CTA	8.2	0.34	1	0.5 M NaCl	[3]
TFC flat-sheet (HTI)	Psf	13	0.81	2	DI	[62]
TFC flat-sheet membrane	Psf	12	0.4	1	10mM NaCl	[63]
TFC flat-sheet membrane	Psf	20.5	–	1	DI	[64]
TFC flat-sheet membrane	Psf	15.1	–	1	DI	[15]

*All results are for FO mode of operation

Acknowledgments

Authors would like to appreciate the Ton Duc Thang University and Aquaporin Asia Pte. Ltd in Singapore for supporting this work and providing the AQP FO membrane, respectively.

Symbols

C_f — NaCl concentration in the feed [$kg{\cdot}m^{-3}$]
C_p — NaCl concentration in permeate [$kg{\cdot}m^{-3}$]
J_s — Reverse solute flux [$g\ m^{-2}\ h^{-1}$]
J_w — Water flux [$L\ m^{-2}\ h^{-1}$]
m — Mass gradient [kg]
m_f — Feed final weight [kg]
Rs — Salt rejections
S_m — Membrane surface area [m^2]
t — Time [h]
W_d — Dry mass of the membrane [kg]
W_w — Wet mass of the membrane [kg]

Greek

Δ — Gradient
ε — Porosity
ρ_{feed} — Feed density [$kg{\cdot}m^{-3}$]
ρ_i — Wetting solvent density [$kg{\cdot}m^{-3}$]
ρ_p — Polymer density [$kg{\cdot}m^{-3}$]
ρ_w — Water density [$kg{\cdot}m^{-3}$]
τ — Tortuosity

References

[1] T.Y. Cath, A.E. Childress, M. Elimelech, Forward osmosis: principles, applications, and recent developments, J. Membr. Sci., 281 (2006) 70–87.
[2] C. Klaysom, T.Y. Cath, T. Depuydt, I.F. Vankelecom, Forward and pressure retarded osmosis: potential solutions for global challenges in energy and water supply, Chem. Soc. Rev., 42 (2013) 6959–6989.
[3] J. Zyaie, M. Sheikhi, J. Baniasadi, S. Sahebi, T. Mohammadi, Assessment of thermally modified cellulose acetate forward osmosis membrane using response surface methodology based on Box-Behnken design, Chem. Eng. Technol., 41(9) (2018) 1706-1715.
[4] H. Aghdasinia, A. Khataee, M. Sheikhi, P. Takhtfiroozeh, Pilot plant fluidized-bed reactor for degradation of basic blue 3 in heterogeneous fenton process in the presence of natural magnetite, Environ. Progr. Sustain. Energy, 36 (2017) 1039–1048.
[5] S. Sahebi, Developing thin film composite membranes for engineered osmosis processes, in, 2015.
[6] S. Zhao, L. Zou, C.Y. Tang, D. Mulcahy, Recent developments in forward osmosis: opportunities and challenges, J. Membr. Sci., 396 (2012) 1–21.
[7] T.-S. Chung, S. Zhang, K.Y. Wang, J. Su, M.M. Ling, Forward osmosis processes: yesterday, today and tomorrow, Desalination, 287 (2012) 78–81.
[8] B. Mi, M. Elimelech, Organic fouling of forward osmosis membranes: fouling reversibility and cleaning without chemical reagents, J. Membr. Sci., 348 (2010) 337–345.
[9] R.J. Aaberg, Osmotic power: a new and powerful renewable energy source?, Refocus, 4 (2003) 48–50.
[10] E.G. Beaudry, J.R. Herron, Direct osmosis for concentrating wastewater, SAE Trans., (1997) 460–466.
[11] K. Popper, W. Camirand, F. Nury, W. Stanley, Dialyzer concentrates beverages, Food Eng, 38 (1966) 102–104.
[12] S. Phuntsho, H.K. Shon, S. Hong, S. Lee, S. Vigneswaran, A novel low energy fertilizer driven forward osmosis desalination for direct fertigation: evaluating the performance of fertilizer draw solutions, J. Membr. Sci., 375 (2011) 172–181.
[13] T. Majeed, S. Sahebi, F. Lotfi, J.E. Kim, S. Phuntsho, L.D. Tijing, H.K. Shon, Fertilizer-drawn forward osmosis for irrigation of tomatoes, Desal. Water Treat., 53 (2015) 2746–2759.
[14] S. Sahebi, S. Phuntsho, J.E. Kim, S. Hong, H.K. Shon, Pressure assisted fertiliser drawn osmosis process to enhance final dilution of the fertiliser draw solution beyond osmotic equilibrium, J. Membr. Sci., 481 (2015) 63–72.
[15] N.Y. Yip, A. Tiraferri, W.A. Phillip, J.D. Schiffman, M. Elimelech, High performance thin-film composite forward osmosis membrane, Environ. Sci. Technol., 44 (2010) 3812–3818.
[16] S. Sahebi, S. Phuntsho, L. Tijing, G. Han, D.S. Han, A. Abdel-Wahab, H.K. Shon, Thin-film composite membrane on a compacted woven backing fabric for pressure assisted osmosis, Desalination, 406 (2017) 98–108.
[17] M.T. Hosseinzadeh, A. Hosseinian, Novel thin film composite nanofiltration membrane using monoethanolamine (MEA) and diethanolamine (DEA) with m-phenylenediamine (MPD), J. Polym. Environ., 26 (2018) 1745–1753.
[18] S. Sahebi, H.K. Shon, S. Phuntsho, B. Ramavandi, Fabricating robust thin film composite membranes reinforced on woven mesh backing fabric support for pressure assisted and forward osmosis: A dataset, Data in Brief, 21 (2018) 364–370.
[19] J. Su, Q. Yang, J.F. Teo, T.-S. Chung, Cellulose acetate nanofiltration hollow fiber membranes for forward osmosis processes, J. Membr. Sci., 355 (2010) 36–44.
[20] J. Su, T.-S. Chung, B.J. Helmer, J.S. de Wit, Enhanced double-skinned FO membranes with inner dense layer for wastewater treatment and macromolecule recycle using Sucrose as draw solute, J. Membr. Sci., 396 (2012) 92–100.
[21] J.R. McCutcheon, M. Elimelech, Influence of membrane support layer hydrophobicity on water flux in osmotically driven membrane processes, J. Membr. Sci., 318 (2008) 458–466.
[22] S. Sahebi, S. Phuntsho, Y.C. Woo, M.J. Park, L.D. Tijing, S. Hong, H.K. Shon, Effect of sulphonated polyethersulfone substrate for thin film composite forward osmosis membrane, Desalination, 389 (2016) 129–136.

[23] Y. Wang, F. Wicaksana, C.Y. Tang, A.G. Fane, Direct microscopic observation of forward osmosis membrane fouling, Environ. Sci. Technol., 44 (2010) 7102–7109.
[24] C. Tang, Y. Zhao, R. Wang, C. Hélix-Nielsen, A. Fane, Desalination by biomimetic aquaporin membranes: Review of status and prospects, Desalination, 308 (2013) 34–40.
[25] Fei Z, H. S, Y. J, X. F, Z. Y, Preparation and characterization of bio-based degradable plastic films composed of cellulose acetate and starch acetate, J. Polym. Environ., 23 (2015) 383–391.
[26] Z. Li, R.V. Linares, S. Bucs, L. Fortunato, C. Hélix-Nielsen, J.S. Vrouwenvelder, N. Ghaffour, T. Leiknes, G. Amy, Aquaporin based biomimetic membrane in forward osmosis: Chemical cleaning resistance and practical operation, Desalination, 420 (2017) 208–215.
[27] K.P. Lee, T.C. Arnot, D. Mattia, A review of reverse osmosis membrane materials for desalination—development to date and future potential, J. Membr. Sci., 370 (2011) 1–22.
[28] R. Modi, R. Mehta, H. Brahmbhatt, A. Bhattacharya, Tailor made thin film composite membranes: potentiality towards removal of hydroquinone from water, J. Polym. Environ., 25 (2017) 1140–1146.
[29] L. Xia, M.F. Andersen, C. Hélix-Nielsen, J.R. McCutcheon, Novel commercial aquaporin flat-sheet membrane for forward osmosis, Ind. Eng. Chem. Res., 56 (2017) 11919–11925.
[30] N. Ma, J. Wei, R. Liao, C.Y. Tang, Zeolite-polyamide thin film nanocomposite membranes: towards enhanced performance for forward osmosis, J. Membr. Sci., 405 (2012) 149–157.
[31] N. Niksefat, M. Jahanshahi, A. Rahimpour, The effect of SiO_2 nanoparticles on morphology and performance of thin film composite membranes for forward osmosis application, Desalination, 343 (2014) 140–146.
[32] A. Tiraferri, Y. Kang, E.P. Giannelis, M. Elimelech, Highly hydrophilic thin-film composite forward osmosis membranes functionalized with surface-tailored nanoparticles, ACS Appl. Mater. Interf., 4 (2012) 5044–5053.
[33] M. Amini, M. Jahanshahi, A. Rahimpour, Synthesis of novel thin film nanocomposite (TFN) forward osmosis membranes using functionalized multi-walled carbon nanotubes, J. Membr. Sci., 435 (2013) 233–241.
[34] H. Zhao, S. Qiu, L. Wu, L. Zhang, H. Chen, C. Gao, Improving the performance of polyamide reverse osmosis membrane by incorporation of modified multi-walled carbon nanotubes, J. Membr. Sci., 450 (2014) 249–256.
[35] D. Emadzadeh, W.J. Lau, T. Matsuura, A.F. Ismail, M. Rahbari-Sisakht, Synthesis and characterization of thin film nanocomposite forward osmosis membrane with hydrophilic nanocomposite support to reduce internal concentration polarization, J. Membr. Sci., 449 (2014) 74–85.
[36] M. Kumar, M. Grzelakowski, J. Zilles, M. Clark, W. Meier, Highly permeable polymeric membranes based on the incorporation of the functional water channel protein Aquaporin Z, Proc. Nat. Acad. Sci., 104 (2007) 20719–20724.
[37] H.C. Visser, D.N. Reinhoudt, F. de Jong, Carrier-mediated transport through liquid membranes, Chem. Soc. Rev., 23 (1994) 75–81.
[38] G. Stark, B. Ketterer, R. Benz, P. Läuger, The rate constants of valinomycin-mediated ion transport through thin lipid membranes, Biophys. J., 11 (1971) 981–994.
[39] Y. Kondo, T. Bührer, E. Frömter, W. Simon, A new double-barrelled, ionophore-based microelectrode for chloride ions, Pflügers Archiv, 414 (1989) 663–668.
[40] V.S. Kislik, Liquid Membranes: Principles and Applications in Chemical Separations and Wastewater Treatment, Elsevier, 2009.
[41] J. Ren, J.R. McCutcheon, A new commercial biomimetic hollow fiber membrane for forward osmosis, Desalination, 442 (2018) 44–50.
[42] G. Sun, H. Zhou, Y. Li, K. Jeyaseelan, A. Armugam, T.-S. Chung, A novel method of Aquaporin Z incorporation via binary-lipid Langmuir monolayers, Colloids Surfaces B: Biointerfaces, 89 (2012) 283–288.
[43] X. Li, R. Wang, C. Tang, A. Vararattanavech, Y. Zhao, J. Torres, T. Fane, Preparation of supported lipid membranes for aquaporin Z incorporation, Colloids Surfaces B: Biointerfaces, 94 (2012) 333–340.
[44] H. Wang, T.S. Chung, Y.W. Tong, K. Jeyaseelan, A. Armugam, Z. Chen, M. Hong, W. Meier, Highly permeable and selective pore-spanning biomimetic membrane embedded with Aquaporin Z, Small, 8 (2012) 1185–1190.
[45] M. Sára, U.B. Sleytr, Production and characteristics of ultrafiltration membranes with uniform pores from two-dimensional arrays of proteins, J. Membr. Sci., 33 (1987) 27–49.
[46] S. Weigert, M. Sára, Surface modification of an ultrafiltration membrane with crystalline structure and studies on interactions with selected protein molecules, J. Membr. Sci., 106 (1995) 147–159.
[47] M. Khajouei, M. Jahanshahi, M. Peyravi, H. Hoseinpour, A.S. Rad, Anti-bacterial assay of doped membrane by zero valent Fe nanoparticle via in-situ and ex-situ aspect, Chem. Eng. Res. Design, 117 (2017) 287–300.
[48] J. Puls, S.A. Wilson, D. Hölter, Degradation of cellulose acetate-based materials: a review, J. Polym. Environ., 19 (2011) 152–165.
[49] G. Sun, T.-S. Chung, K. Jeyaseelan, A. Armugam, A layer-by-layer self-assembly approach to developing an aquaporin-embedded mixed matrix membrane, RSC Adv., 3 (2013) 473–481.
[50] G. Sun, T.-S. Chung, K. Jeyaseelan, A. Armugam, Stabilization and immobilization of aquaporin reconstituted lipid vesicles for water purification, Colloids Surfaces B: Biointerfaces, 102 (2013) 466–471.
[51] G. Sun, T.-S. Chung, N. Chen, X. Lu, Q. Zhao, Highly permeable aquaporin-embedded biomimetic membranes featuring a magnetic-aided approach, RSC Adv., 3 (2013) 9178–9184.
[52] S. Loeb, L. Titelman, E. Korngold, J. Freiman, Effect of porous support fabric on osmosis through a Loeb-Sourirajan type asymmetric membrane, J. Membr. Sci., 129 (1997) 243–249.
[53] Y. Zhao, C. Qiu, X. Li, A. Vararattanavech, W. Shen, J. Torres, C. Hélix-Nielsen, R. Wang, X. Hu, A.G. Fane, C.Y. Tang, Synthesis of robust and high-performance aquaporin-based biomimetic membranes by interfacial polymerization-membrane preparation and RO performance characterization, J. Membr. Sci., 423–424 (2012) 422–428.
[54] T. Hu, X. Wang, C. Wang, X. Li, Y. Ren, Impacts of inorganic draw solutes on the performance of thin-film composite forward osmosis membrane in a microfiltration assisted anaerobic osmotic membrane bioreactor, RSC Adv., 7 (2017) 16057–16063.
[55] Y. Chun, L. Qing, G. Sun, M.R. Bilad, A.G. Fane, T.H. Chong, Prototype aquaporin-based forward osmosis membrane: Filtration properties and fouling resistance, Desalination, 445 (2018) 75–84.
[56] M. Qasim, N.A. Darwish, S. Sarp, N. Hilal, Water desalination by forward (direct) osmosis phenomenon: A comprehensive review, Desalination, 374 (2015) 47–69.
[57] Y.-x. Shen, P.O. Saboe, I.T. Sines, M. Erbakan, M. Kumar, Biomimetic membranes: A review, J. Membr. Sci., 454 (2014) 359–381.
[58] S. Phuntsho, S. Sahebi, T. Majeed, F. Lotfi, J.E. Kim, H.K. Shon, Assessing the major factors affecting the performances of forward osmosis and its implications on the desalination process, Chem. Eng. J., 231 (2013) 484–496.
[59] G.T. Gray, J.R. McCutcheon, M. Elimelech, Internal concentration polarization in forward osmosis: role of membrane orientation, Desalination, 197 (2006) 1–8.
[60] K.Y. Wang, T.S. Chung, G. Amy, Developing thin-film-composite forward osmosis membranes on the PES/SPSf substrate through interfacial polymerization, AIChE J., 58 (2012) 770–781.
[61] C. Bae, K. Park, H. Heo, D.R. Yang, Quantitative estimation of internal concentration polarization in a spiral wound forward osmosis membrane module compared to a flat sheet membrane module, Korean J. Chem. Eng., 34 (2017) 844–853.
[62] W.A. Phillip, J.S. Yong, M. Elimelech, Reverse draw solute permeation in forward osmosis: modeling and experiments, Environ. Sci. Technol., 44 (2010) 5170–5176.
[63] J. Wei, C. Qiu, C.Y. Tang, R. Wang, A.G. Fane, Synthesis and characterization of flat-sheet thin film composite forward osmosis membranes, J. Membr. Sci., 372 (2011) 292–302.
[64] A. Tiraferri, N.Y. Yip, W.A. Phillip, J.D. Schiffman, M. Elimelech, Relating performance of thin-film composite forward osmosis membranes to support layer formation and structure, J. Membr. Sci., 367 (2011) 340–352.